ELSEVIER

International Journal of Pharmaceutics 167 (1998) 129–138

international journal of pharmaceutics

Assessing the particle size of a broadly dispersed powder by complementary techniques

C. Andrès [a,*], P. Bracconi [b], P. Réginault [c], P. Blouquin [c], M.H. Rochat [a], Y. Pourcelot [a]

[a] *Technological Group on Pharmaceutical Powders, School of Pharmacy, University of Burgundy, 7 Bd Jeanne d'Arc, 21033 Dijon, France*

[b] *Laboratory for the Reactivity of Solids, University of Burgundy, 9 avenue Alain Savary, B.P. 400, 21011 Dijon Cedex, France*

[c] *Research and Development, Fournier Laboratories SCA, 50 rue de Dijon, 21121 Daix, France*

Received 6 October 1997; received in revised form 15 January 1998; accepted 18 January 1998

Abstract

The experimental determination of reliable particle size distribution curves and statistical parameters of broad distributions is known to be a difficult task. This problem is addressed here in an attempt to characterize the granularity of three distinct batches of a pharmaceutical powder (fenofibrate from Fournier Laboratories). The methodology consists in comparing the results, expressed in terms of surface based mean diameter, as obtained by three complementary techniques, namely optical microscopy image analysis, laser light low angle diffraction and surface area measurement by krypton physisorption. These techniques are applied in parallel to the material of interest and to a certified reference material, a nearly spherical and narrowly distributed glass powder. © 1998 Elsevier Science B.V. All rights reserved.

Keywords: Image analysis; Laser light diffraction; Krypton physisorption; Particle-size distribution

1. Introduction

Today, the pharmaceutical industry pays much attention to the role and variability of the physical properties of particulate materials, not only active ingredients, but also excipients. In the rapidly growing field of pharmaceutical powder technology and solid dosage forms, particle size and shape are known to affect the product performances including processing characteristics, content uniformity, stability as well as solubility and bioavailability, and consequently therapeutic efficiency. Many techniques for the measurement of particle size are available, but their choice and

* Corresponding author.

0378-5173/98/$19.00 © 1998 Elsevier Science B.V. All rights reserved.
PII S0378-5173(98)00052-0

application may prove difficult, and one has to resort to and compare the results from different ones to better assess the powder granular properties and the consequences on its functionality.

Most often a powder is composed of three types of particles, elementary particles, aggregates and agglomerates and offers a variety not only of particle sizes, but also of particle shapes. For the purpose of size analysis, a particle is reduced to a geometrical object characterized by its volume (proportional to weight), the area of its interface with the dispersion medium and its specific linear dimensions (length, width, thickness, diameter). All these parameters are measurable, keeping in mind that the definitions of size and shape are strongly interdependent. In fact, only seldom can the actual geometrical characteristics of a particle be strictly expressed in the value of a single dimensional parameter. Most often, one is faced with the necessity of assigning more or less arbitrarily a basic geometrical shape to the particle and then calculate a so called equivalent dimensional parameter, e.g. equivalent diameter if the sphere model is used.

Practically, a particle-size distribution is characterized by two dimensions: the dimensional factor and the frequency (the latter being a number, a weight, a volume or an area, depending on the applied technique). Consequently, the results obtained through different techniques cannot be directly compared unless they are presented in the same dimensionality (Besançon et al., 1990).

By then, it is essential to precisely understand the physical principle on which the utilised technique is based, as well as its main specifications, implications and limits. Many methods are now available (Washington, 1992) based on many different principles and materials physical properties such as, for example, optical (laser diffraction), densitometric (sedimentograph), electrical (Coulter counter) etc.. All of them may be limited in a particular application either by some specific property of the investigated material or by the use of a reducing model of particle shape and they differ by the analyzed size range, resolution, size and ease of preparation of the sample and by whether the particles are counted and measured individually or not.

The purpose of the present work is to describe and compare the results of different techniques of measurement of the distribution and mean value of particle size, namely laser light diffraction (LD), image analysis (IA) and physisorption of krypton (Ads) as they are applied to a bulk pharmaceutical powder with broad particle size distribution (in the 1–1000 μm range) and non spherical shape. The methodology of comparison consists in reducing all data to a single common statistical parameter the choice of which is determined by the least informative of the utilized techniques and based on the knowledge of the dimensionality of the results they provide.

2. Materials and techniques

Three 100-g batches of fenofibrate, a pharmaceutical active drug from Fournier Laboratories, are analysed in the present work. They are referred to as P1, P2 and P3 in the following. As they were taken from the production line at different dates, differences in their granular properties may eventually result from unintended fluctuations of the raw materials properties and/or processing parameters.

A reference glass powder (RGP in the following) is also systematically analysed. It is made of nearly spherical particles with diameters in the range 6–60 μm. It is the reference standard material # 1003b from the National Institute of Standards and Technology (NIST) and its number and volume based particle size distributions are known.

The value of the density, ρ, of these fenofibrate batches is required in Eq. (1) in order to compute the surface based particle diameter, μ_2, from the specific surface area, S_p, of the three batches. As no such value is available in the literature, it is measured here by helium pycnometry (Ultrapycnometer, Quantachrome). The measurements are optimized by using large sample and cell volumes, thorough purging and thermal stabilisation of the pycnometer and by performing 20–30 pressure cycles on each batch.

$$S_p = 6/[\rho\mu_2] \quad (1)$$

The specific surface areas of the fenofibrate batches and RGP are measured by krypton adsorption at liquid nitrogen temperature (Autosorb 1C from Quantachrome). The $0.1 < P/P_0 < 0.6$ section of the isotherms are analysed by the BET theory. The BET theory is known to correctly model the initial section of adsorption isotherms on a majority of non porous and mesoporous solids. When nitrogen is used as adsorbate other theories can also provide similar results. However, there is no such alternative in the case of krypton adsorption which in turns is a requisite for measuring low specific surface areas. The computation of S_{BET} involves the adsorbate saturation vapour pressure, P_0, and molecular cross sectional area for which different sets of values are recommended in the literature (Ranck and Teichner, 1967; Lowell and Shields, 1984). In the present application different combinations have been tested. First, the saturation vapour pressure has been monitored with each adsorption point, but this leads to the largest dispersion of the adsorption isotherm and surface area value from different experiments on a given sample (around 10%). Much better reproducibility was obtained by using a single P_0 value, here set to 2.27 mbar, characteristic of solid krypton. Accordingly the molecular cross sectional area was set to 0.215 nm^2 (Ranck and Teichner, 1967).

Image analysis is carried out using a system built from an optical microscope model NS 400 from Nachet, a CCD camera model 4712-5000 from Cohu and the treatment and image analysis software Vidas from Kontron. The as captured images are sharply contrasted, showing well isolated particles. Consequently, they require no particular morpho-mathematical treatment prior to binarisation (e.g. erosion-dilatation). They are directly digitized in 512×512 pixels, 256 grey levels and exhibit a final numerical resolution of 1 μm per pixel. One may mention here that a few additional examinations were also performed at a higher magnification corresponding to a numerical resolution of 0.1 μm per pixel in an effort to determine with some accuracy the low limit of the particle size range.

For each batch at least 500 particles are analysed. Since the particles have a compact shape, the equivalent projection area diameter is the most pertinent dimensional parameter. It is simply referred to as the IA diameter and noted d_p in the following. The surface-based mean diameter μ_2 is calculated from the number distribution of the IA diameter by:

$$\mu_2 = \Sigma\, n_i d_p^3 / \Sigma\, n_i d_p^2 \quad (2)$$

As for particle size measurement by laser light diffraction (LD), the Coulter LS130 analyser from Coultronics is used. Analyses are carried out on the three fenofibrate batches in suspension in air (LD-PIA, using the so called dry powder module) and in suspension in liquid (LD-PIL, using the so called standard liquid module). The RGP is analysed exclusively by LD-PIL because LD-PIA requires material amounts larger than available. For LD-PIA, the drive parameters are set to 30 s acquisition time, 8–12% obscuration and three trials are run for each batch on 10–15 g samples. For LD-PIL, analyses are run on 1 l of distilled water added with 2 ml of Nonarox (20 vol%), and drive parameters are set to 30 s acquisition time, 4–8% for obscuration and three trials are run for each batch on 2–4 g samples. Since no reliable value of the fenofibrate refractive index is available in the literature, and, more importantly, because in the size range of concern here the Mie theory may lead to unstable solutions (due to difficulties with the numerical evaluation of Ricatti-Bessel functions), diffraction data are treated according to the more robust far field Fraunhofer theory. Additional results obtained with the RGP are presented in Appendix A to illustrate these difficulties. They emphasize the need for a very precise and independent knowledge of the refraction index of materials when applying more sophisticated theories such as Mie's (shown here) to scattering data.

The surface based mean diameter μ_2 is here calculated from the LD volume distribution by

$$\mu_2 = \Sigma\, v_i / \Sigma\, [v_i / d_i] \quad (3)$$

where v_i stands for the volume frequency, and d_i for the mean diameter of class i.

As will appear obvious from the following, the only consistent way by which the results from the above techniques can be compared is dictated by

Table 1
Fenofibrate density and surface area values as measured by helium pycnometry and krypton adsorption (corresponding 95% confidence intervals are indicated)

	Batch		
	P1	P2	P3
Density ($g\ cm^{-3}$)	1.24949 ± 0.00007	1.24944 ± 0.00006	1.24952 ± 0.00007
Pressure cycles	29	30	24
Surface area ($m^2\ g^{-1}$)	0.152 ± 0.007	0.146 ± 0.004	0.139 ± 0.002
Number of experiments	3	3	3

considerations of statistical and technical nature. The direct comparison of the distributions obtained from IA and LD will prove impracticable and the only valuable overall comparison of the three techniques will concern the surface based mean diameter.

3. Results and discussion

3.1. Densities and surface areas

The three fenofibrate batches do not show any significant difference in density (Table 1). The average of the three measured values, namely 1.2495 g cm^{-3}, should constitute a reference since, to the authors present knowledge, no such data can be found in the literature.

The specific surface area values shown in Table 1 vary only slightly from one batch to the other. The value observed for P3 is significantly lower (from a statistical standpoint) than those for P1 and P2 which in turn may be considered identical within a margin error of 5%.

3.2. Image analysis

An optical micrograph of particles from batch P1 is presented in Fig. 1a. The particles are obviously broadly dispersed in size and of irregular, though rather compact, shape. Accordingly they have a certain surface roughness (which we do not attempt to characterize further). In comparison, the RGP is relatively close to a monodispersion of spherical particles (see Fig. 1b).

As shown in Fig. 2, the number distributions of the particle diameter obtained by IA for the three batches are almost superimposable between 4–400 μm, which constitutes the range of the actually observed diameters. In contrast to the RGP

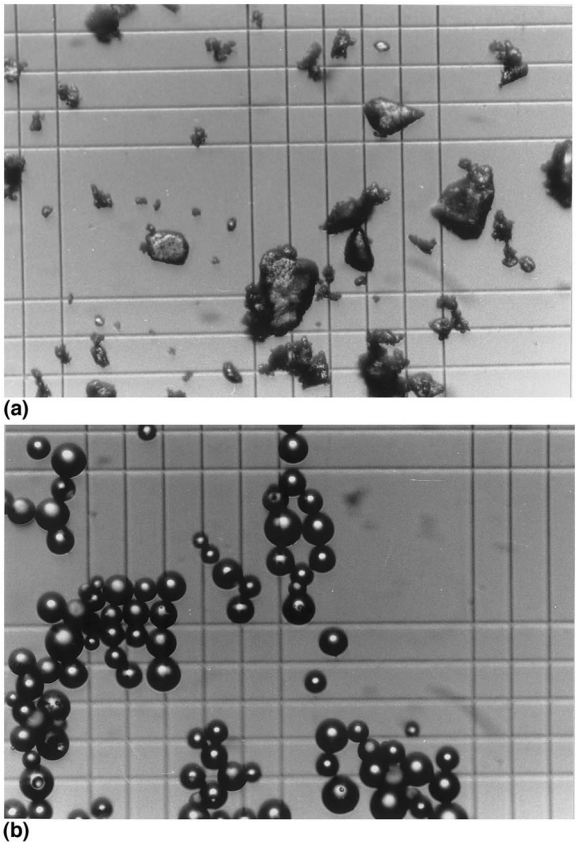

Fig. 1. Optical microscopy images of particles from (a) fenofibrate batch and (b) the RGP. The small squares of the grid have 50 μm edge length.

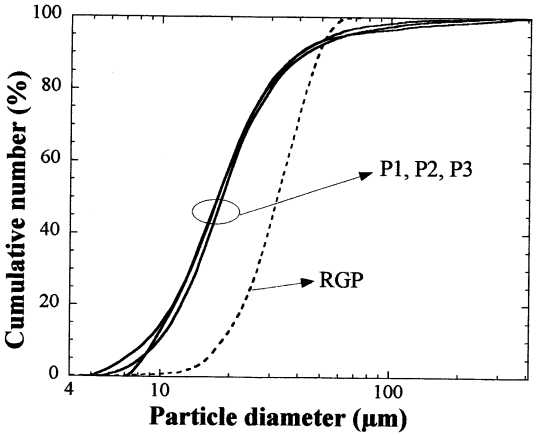

Fig. 2. Cumulative number distribution curves obtained by IA.

curve, they exhibit a long tail at high diameter values. The different values of the statistical parameters namely quantiles, geometric mean and geometric standard deviation, are very close (Table 2). In particular the range of variation of the geometrical mean is strikingly narrow: 18.9–19.9 μm and just equal to the numerical resolution of the analysed images.

3.3. Laser light diffraction

The volume distribution curves obtained by laser light diffraction are presented in Fig. 3a and b. Obviously, the particle populations are broadly dispersed over the almost entire experimentally accessible range (0.4–900 μm). All distributions show three distinct modes: the first one, very weak, around 1 μm, the second one around 30 μm, and the third one between 200–300 μm which in two cases turns to be the main mode. The RGP distribution curve obtained by LD-PIL is also shown in Fig. 3b and proves much narrower.

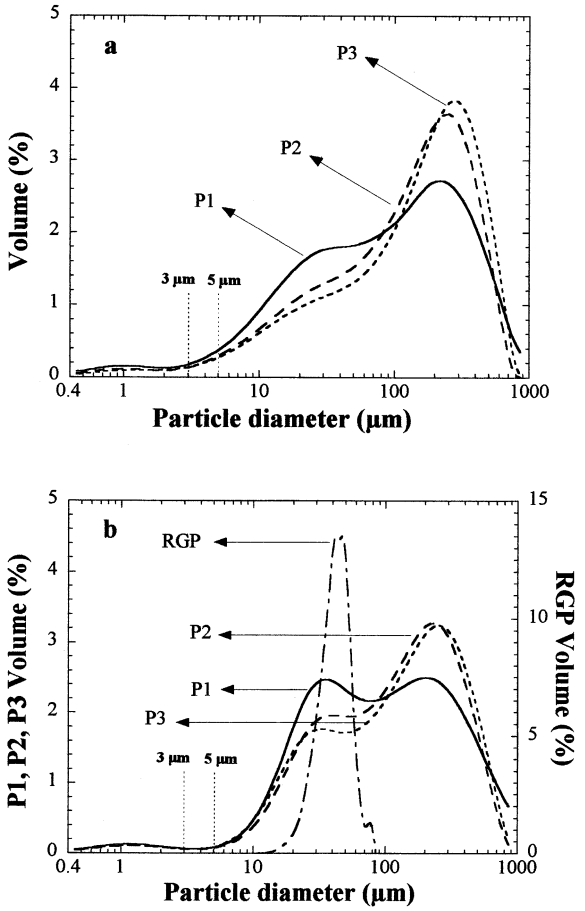

Fig. 3. Volume distribution curves obtained by laser diffraction, (a) in air LD-PIA, (b) in liquid LD-PIL.

Table 2
Main statistical parameters of number distributions of diameter from IA

	Batches		
	P1	P2	P3
Number	513	560	545
$d_{0,10}$ (μm)	9.4	9.2	10.2
$d_{0,50}$ (μm)	17.7	17.5	18.4
$d_{0,90}$ (μm)	39.4	37.9	42.1
G_0 (μm)	18.9	19.0	19.9
GSD_0	1.8	2.0	1.8

$d_{i,j}$, Quantiles of diameter distribution, with i being the frequency dimension (0 for a number frequency) and j being the percentile (for example 10 for the tenth percentile).
G_0, geometric mean.
GSD_0, geometric standard deviation.

The presence of the first mode is in clear contradiction with the above optical microscopy observations and image analysis results which show no particles with diameters lower than 4–5 μm even when operating at the highest resolution of 0.1 µm per pixel. Indeed, the number distributions

Table 3
Main statistical parameters of the diameter distributions obtained by laser diffraction (corresponding 95% confidence intervals are indicated)

Statistical parameter	Technique	P1	P2	P3
$d_{3,10}$ (μm)	LD-PIA	14.6 ± 0.6	18.4 ± 1.7	20.1 ± 2.5
	LD-PIL	20.9 ± 0.6	23.1 ± 1.0	21.6 ± 0.7
$d_{3,50}$ (μm)	LD-PIA	105.0 ± 10.3	148.2 ± 16.6	176.6 ± 23.4
	LD-PIL	96.2 ± 3.4	132.8 ± 1.7	141.4 ± 8.8
$d_{3,90}$ (μm)	LD-PIA	408.3 ± 31.4	392.1 ± 19.7	408.3 ± 31.4
	LD-PIL	427.3 ± 19.6	404.8 ± 12.8	427.3 ± 19.6
G_3 (μm)	LD-PIA	87.6 ± 6.4	109.8 ± 10.7	127.3 ± 15.0
	LD-PIL	93.3 ± 2.5	109.8 ± 1.7	113.2 ± 4.8
GSD_3	LD-PIA	3.49 ± 0.05	3.19 ± 0.04	3.22 ± 0.08
	LD-PIL	3.14 ± 0.06	2.95 ± 0.09	3.11 ± 0.02

$d_{i,j}$, Quantiles of diameter distribution with i being the frequency dimension (3 for a volume frequency) and j being the percentile (for example 10 for the tenth percentile).
G_3, geometric mean of volume diameter distribution.
GSD_3, geometric standard deviation of volume diameter distribution.

(not shown) computed from the volume distributions of Fig. 3a and b are 'j' shaped curves asymptotic to the vertical $D = 0.4$ μm indicating a majority of 0.4 μm particles, which obviously is physically inconsistent. Clearly, this first mode does not provide a reliable estimation of the size distribution of the finest particles. It may result from approximations inherent to the Fraunhofer theory, and/or be a mathematical artifact of the constrained numerical inversion procedure of the raw diffracted intensity data. Consequently, only the particles larger than 4 μm in diameter (i.e. larger than the smallest particles detected by IA) are taken into consideration in the computation of the statistical parameters values appearing in Tables 3 and 4.

The comparison of the distributions of the three batches measured in air (Fig. 3a) and in water (Fig. 3b) reveals that P2 and P3 are again very similar, whereas P1 is composed of smaller particles.

When the results from the LD-PIA and LD-PIL techniques in Fig. 3a and b are compared batch to batch, one may observe that the amplitude of the second mode (20–30 μm) always proves higher in LD-PIL distributions. The geometric mean diameter should shift accordingly. In addition, LD-PIL measures a comparatively lower amount of fine particles around 4 μm (i.e. at and just above the minimum of the distributions between the first and second peaks).

However, the comparison of the $d_{3,90}$ values (Table 3) points out that a higher ratio of large particles is systematically obtained by LD-PIL. This can tentatively be explained by insufficient particles deagglomeration in water in relation with the well known hydrophobic properties of fenofribrate. On the whole, for LD-PIL, the higher amplitude of the second mode (20–30 μm) relative to LD-PIA, the relative lack of 4 μm particles and the higher ratio of large particles apparently all compensate each other in the final estimate of the geometric mean of the particles diameter (Table 3) since the values from LD-PIL and LD-PIA never differ by more than 12.5%.

As a conclusion, one can emphasize the two following major differences in particle-size distribution analysis by LD-PIA and LD-PIL: LD-PIL underestimates the population of small particles as is particularly noticeable in the range 3–5 μm in Fig. 3a and b, and incorrectly estimates the populations of large particles presumably because of insufficient deagglomeration. So, LD-PIA seems to be better adapted to the measurement of the size distribution of the present material and the results from LD-PIL will not be used in the following when comparing LD to IA and Ads. Nevertheless, both techniques provide the same

Table 4
Estimations of mean diameters μ_2 by krypton adsorption, IA and PIA (corresponding 95% confidence intervals are indicated)

	Batch				Span[a]
	RGP	P1	P2	P3	
Ads	43 ± 1	31.6 ± 1.3	32.9 ± 1.6	34.5 ± 0.6	10%
IA	42 ± 1	20.3 ± 6.3	21.5 ± 4.2	21.7 ± 4.5	Not significant
LD-PIA	39 ± 1	35.4 ± 1.6	44.8 ± 3.6	48.5 ± 4.9	35%

[a] Measured by $[\mu_2(P3)-\mu_2(P1)]/\mu_2(P2)$.

hierarchy of geometric mean particle diameter for the three investigated batches (Table 3):

$$G(P1) < G(P2) < G(P3)$$

3.4. Comparison of results from the different techniques

As mentioned in Section 1, in order to compare the results from the different techniques, krypton physisorption, optical image analysis and laser light diffraction, it is necessary to turn all the results into a single representation. In the present case, the least informative technique is the measure of specific surface area which can provide only a mean parameter, not a distribution. As long as only the surface area value is considered, no assumption on particle shape is required. This is no longer true when one wants to compute the value of a dimensional parameter from the surface area value. If a model of spherical particle is considered, in agreement with the same assumption made in the analysis of the optical microscopy images and laser diffraction results, μ_2 is readily obtained from Eq. (1).

IA and LD-PIA provide two other independent estimations of μ_2 given by Eqs. (2) and (3). The three sets of data are compared in Table 4 and the comparison is extended to the RGP.

On the whole, when comparing the different estimators of μ_2 in Table 4, the three techniques allow to classify the fenofibrate batches according to the same hierarchy:

$$\mu_2(P1) < \mu_2(P2) < \mu_2(P3)$$

However, based on the relative span of the data from a given technique, this increase is not significant for IA, quite low for adsorption and comparatively strong for LD-PIA.

In contrast to the RGP, each one of the three fenofibrate batches exhibits significant differences between the μ_2 estimates from the different techniques and, as discussed now, this is directly or indirectly related to the very different widths of the particle size distributions of the two materials and, to a lesser extent, to a more irregular particle shape of the fenofibrate particles.

Vapour adsorption is the only technique which allows a direct measurement of true specific surface area, i.e. without any hypothesis about particle shape, and taking into account surface roughness (which may significantly enhance the final result). The choice of the sphere as a shape model minimizes the estimate of μ_2 from krypton adsorption since the sphere is the geometrical object with the lowest surface area per unit volume. Accordingly, as a result of the observed surface roughness and asphericity (obvious though not quantitatively assessed in Fig. 1a), all other techniques, here IA and LD, resorting to the sphere model, should provide an estimate of μ_2 either higher or equal to the value calculated from gas adsorption.

This is at variance with the results in Table 4 since the estimates of μ_2 by IA are always lower than those from krypton adsorption. Such a contradiction can be understood by expressing the estimation errors on particle-size distribution from IA in terms of surface frequency. Indeed, in this case the principle stated by Paine (1993) can be applied: a critical number of particles, N_{crit}, must be measured to allow a sensible estimation of the center position measure parameter of the distribution expressed in terms of area frequency.

This critical number is related to the true geometric standard deviation GSD_2 of the distribution by:

$$N_{crit} = \exp[1.71 \exp[0.5r] \times (GSD_r - 0.83)] \quad (4)$$

r being the dimensionality of the frequency of the target distribution.

Table 5 shows the values of N_{crit} that can be calculated by Eq. (4) based on the GSD_2 values computed from the results of the LD-PIA technique which are the only independent available estimates. They are indeed 100–1000 times larger than the number of particles actually observed but are also not achievable with the image analysis equipment used in the present work. According to Paine (1993), since the number of analysed particles is too small, the μ_2 values of the IA distributions in Table 4 are necessarily smaller than the true unknown value, which points to the fact that a significant number of large (i.e. with low number frequency) particles must have escaped observation. In contrast, the narrow distribution of the RGP could in principle be assessed from a much lower number of observations.

As a conclusion, it is clear that the present application of image analysis is unable to provide a reliable estimation of μ_2 for a wide dispersion of particle dimensions and one can state that the observed differences between the μ_2 estimates by krypton adsorption and image analysis are essentially the result of the small number of particles counted by IA.

The estimates of μ_2 by LD-PIA are always larger than those obtained by krypton adsorption (Table 4). This now is in accordance with the implication of the choice of the sphere as a shape model and with the particles surface roughness.

Table 5
Estimations of GSD_2 from LD-PIA and Paine's critical number N_{crit} (corresponding 95% confidence intervals are indicated)

	Batch			
	RGP	P1	P2	P3
GSD_2	1.45 ± 0.07	3.16 ± 0.06	3.58 ± 0.14	3.76 ± 0.20
N_{crit}	18	50 000	360 000	800 000

Nevertheless, one should not overlook the fact that it may also partly result from the way the first mode of the raw distributions is subtracted: compared to a hypothetical numerical desummation the simple rejection of the population finer than 4 μm certainly contribute to a slight overestimation of μ_2.

Finally, the differences between the estimates of μ_2 by LD-PIA and LD-PIL point to and may tentatively be explained by the possible dissolution of the fenofibrate in the dispersion medium.

4. Conclusion

In a previous paper (Andrès et al., 1996) an ideal system of spherical particles has been investigated and the importance of a proper choice of a frame of comparison of the results from different techniques to measure particle size was emphasized. Most methods make the basic assumption (explicitly or implicitly) that the particles are spherical thus making it difficult, as shown in the present paper, to evaluate a broad particle size distribution from a limited sample of a non spherical powder.

Today one can observe the growing utilisation of laser diffraction methods in particle size analysis. It is shown here that LD-PIA is indeed an efficient, simple and reliable technique for evaluation of batch to batch variability of a relatively coarse powder (above 10 μm). Evidence is also provided that an accurate value of the real part of the complex refractive index is mandatory if one wants to analyse very fine powders (say below a few μm) by taking advantage of theories more elaborate than Fraunhofer's.

Some information on the particles shape is uniquely given by IA, but this method also has its drawbacks. Not mentioning lengthy analyses, it considers only projected images and equivalent projection area diameters, and, especially when broad distributions are concerned, there is a critical number of particles to be counted so as to ensure reliable results that can be considerable and even unachievable at acceptable costs.

The methodology followed in the present work has the advantage of resorting to the utilisation of

a minimum number of techniques to allow the measurement of the basic granular properties of a broadly dispersed non-spherical powder and the simultaneous assessment of the error potentially linked to that dispersion and to the particle asphericity and surface roughness as well as to the possible reactivity of the powder with a dispersion medium.

Appendix A

The intensity of the light (wavelength λ) scattered by a single sphere of radius a depends on the size parameter $\alpha = 2\pi a/\lambda$, and relative refractive index n_r. As outlined by Kerker (1969), at a particular scattering angle θ, the intensity increases rapidly up to a maximum value at about $\alpha = 2$ and then oscillates in a complicated fashion as the size increases further. The angular positions of the successive minima and maxima shift towards higher values as n_r increases. As a consequence and for a given diffraction pattern, underestimating the value of n_r would result in an underestimation of a. For a distribution of particle sizes the situation is more complicated. The numerical inversion of the Fredholm type integral equation of the scattered intensity is a so called ill-defined mathematical problem, the solution of which involves various constrains generally unknown to the final user of the particle size analyser. Thus, it is practically impossible to appreciate the impact of an error on the value of n_r on the final particle size distribution, based on fundamental considerations. In contrast, it proves very simple to investigate the response of the granulometer to imposed variations of the refractive index value.

We present below the result of such an investigation applied to the RGP. From the given cumulative number and volume distributions provided by the certification sheet from the NIST one gets the following central values: the medians are between 26–28 μm (number based) and 36–38 μm (volume based), the geometrical means are 25.73 μm and 35.83 μm, respectively.

The analyses have been carried out with the LS130 using optical models based on the Mie theory that requires a complex refractive index. As a prototype insulator glass should be characterized by an infinitely small imaginary part n(Im). Indeed assigning the sequence of values $n(\mathrm{Im}) = 0$, 0.001 and 0.01 only results in a very slight shift of the computed distribution function along the a axis. This is of no real practical interest and is no longer considered in the following. As for the real part n(Re) at the actual wavelength of the laser light used, 750 nm, to which glass is fully transparent, the most accurate estimate is in between 1.50 and 1.53. With water as a liquid vector, the real part of the relative refractive index is thus estimated at 1.137 ± 0.012.

A sequence of optical models was built (using the software option of the LS130) with n(Re) increasing from 1.12 to 1.16 by steps of 0.002 to include the above estimation. The computed number based geometrical mean values, G_0, for two distinct experiments are plotted versus n(Re) in Fig. A1. For comparison the volume based geometrical mean values, G_3, have been plotted too. The corresponding values computed from the NIST distribution appear as dotted lines.

All two sets of data appear to be oscillatory functions of n(Re) and show a slightly decreasing overall trend with increasing n(Re), that most likely corresponds to the one expected from above considerations for scattering by a single sphere. The amplitude of the oscillations is strongly decreasing from G_0 to G_3. Most measured values are larger than the corresponding NIST data but the

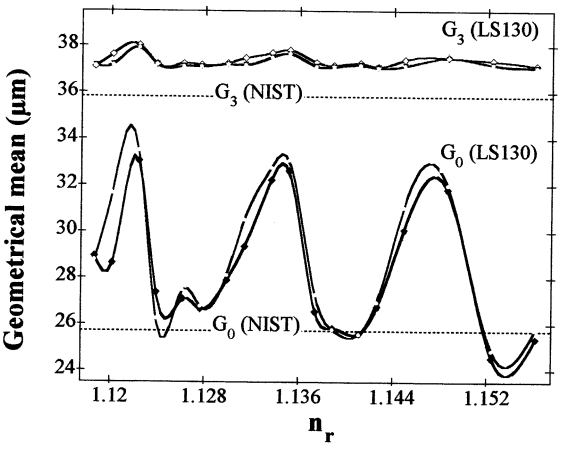

Fig. A1. Dependence on n(Re) of number based (lower curves) and volume based (upper curves) geometric mean diameter.

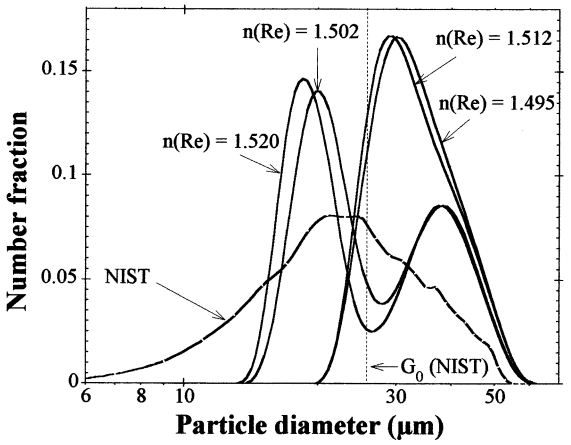

Fig. A2. Number based distributions computed with different refractive index real part values and compared to the NIST images analysis reference distribution.

volume based data are in rather steady excess of 4.1% on the average.

In addition, it appears that the computed number based distribution oscillates between two rather stable monomodal and bimodal functions of the particle diameter (Fig. A2). The bimodal solutions turn to correspond to the minimum values of G_0 in Fig. A1 and to provide the geometrical mean values the closest to the NIST reference.

Nevertheless, they prove physically inconsistent. In conclusion, it appears that a refinement of the technique based on more elaborate theoretical grounds may turn to be impracticable.

References

Andrès, C., Réginault, P., Rochat, M.H., Chaillot, B., Pourcelot, Y., 1996. Particle-size distribution of a powder: comparison of three analytical techniques. Int. J. Pharm. 144, 141–146.

Besançon, P., Chastang, J., Lafaye, A., Lafaye, J.M., 1990. Conversion dimensionnelle des distributions granulométriques. Powder Technol. 60, 205–214.

Kerker, M., 1969. The Scattering of Light and Other Electromagnetic Radiations. In: Loebl, E.M. (Ed.), Physical Chemistry, vol. 16, Academic Press, New York.

Lowell, S., Shields, J.E., 1984. Langmuir and BET theories. In: Lowell, S., Shields, J.E. (Eds.), Powder Surface Area and Porosity, Chapman and Hall, New York, pp. 14–28.

Paine, A.J., 1993. Error esimates in the sampling from particle size distributions. Part. Part. Syst. Charact. 10, 26–32.

Ranck, R.E., Teichner, S.J., 1967. Détermination des surfaces spécifiques par adsorption de krypton. J. Chim. Phys. 2, 401–402.

Washington, C., 1992. Basic principles. In: Washington, C. (Ed.), Particle Size Analysis in Pharmaceutics and Other Industries, Ellis Horwood, New York, pp. 9–39.